Biochimica et Biophysica Acta 1803 (2010) 1028–1037

Contents lists available at ScienceDirect

Biochimica et Biophysica Acta

journal homepage: www.elsevier.com/locate/bbamcr

Identification of an atypical peptidyl-prolyl *cis*/*trans* isomerase from trypanosomatids☆

Esteban D. Erben [a], Ezequiel Valguarnera [a], Sheila Nardelli [b], Janete Chung [b], Sebastian Daum [c], Mariana Potenza [a], Sergio Schenkman [b], María T. Téllez-Iñón [a,*]

[a] Instituto de Investigaciones en Ingeniería Genética y Biología Molecular (INGEBI-CONICET) Buenos Aires, R. Argentina
[b] Departamento de Microbiologia, Imunologia e Parasitologia, Universidad Federal de São Paulo, São Paulo, Brazil
[c] Max Planck Research Unit Enzymology of Protein Folding, Halle, Germany

ARTICLE INFO

Article history:
Received 22 December 2009
Received in revised form 30 April 2010
Accepted 17 May 2010
Available online 24 May 2010

Keywords:
Peptidyl-prolyl *cis*/*trans* isomerase
Parvulin
Pin1-type PPIase
Par45

ABSTRACT

The parvulin family of peptidyl-prolyl *cis*/*trans* isomerases (PPIases) catalyzes the *cis*/*trans* isomerization of the peptide bonds preceding Pro residues. Eukaryotic parvulin-type PPIases have been shown to be involved in cell proliferation and cell cycle progression. Here we present the biochemical and molecular characterization of a novel multi-domain parvulin-type PPIase from the human pathogenic *Trypanosoma cruzi*, annotated as *Tc*Par45. Like most other parvulins, Par45 has an N-terminal extension, but, in contrast to human Pin1, it contains a forkhead-associated domain (FHA) instead of a WW domain at the N-terminal end. Par45 shows a strong preference for a substrate with the basic Arg residue preceding Pro (Suc-Ala-Arg-Pro-Phe-NH-Np: $k_{cat}/K_M = 97.1$ /M/s), like that found for human Par14. In contrast to human Pin1, but similarly to Par14, Par45 does not accelerate the *cis*/*trans* interconversion of acidic substrates containing Glu-Pro bonds. It is preferentially located in the parasite nucleus. Single RNA interference (RNAi)-mediated knock-down showed that there was a growth inhibition in procyclic *Trypanosoma brucei* cells. These results identify Par45 as a phosphorylation-independent parvulin required for normal cell proliferation in a unicellular eukaryotic cell.

1. Introduction

Proline is exceptional in the sphere of amino acids in its ability to adopt *cis* and *trans* conformations, which allows a protein backbone switch that is controlled by prolyl *cis*/*trans* isomerization [1]. Many of the biological events that occur under strict time control, such as the eukaryotic cell cycle and cell proliferation, are affected by the catalytic action of peptidyl-prolyl *cis*/*trans* isomerases (PPIases, EC 5.2.1.8) (Reviewed in [2]). PPIases are ubiquitous enzymes that can abolish slow kinetic phases in protein folding by accelerating *cis*/*trans* isomerization of peptide bonds preceding a proline residue within a polypeptide chain. Based on inhibitor susceptibility and sequence homology, PPIases have been divided into three distinct classes: the cyclosporin A (CsA)-binding proteins (cyclophilins), the FK506-binding proteins (FKBPs) and the parvulins, which do not bind any immunosuppressant drugs [3].

A key breakthrough in appreciating the significance of conformational changes was the discovery of the parvulin-type PPIase Pin1 [4]. This parvulin is a prolyl isomerase that specifically isomerizes the phosphorylated Ser/Thr-Pro bonds regulating the function of mitotic phosphoproteins [5–7]. Pin1 binds proteins that have been phosphorylated by Pro-directed kinases such as cyclin-dependent kinases (CDK) and mitogen-activated protein kinases (MAPK), and induces a conformational change to regulate their function by triggering a programmed set of cell cycle events [4,8].

On the basis of substrate specificity, the eukaryotic parvulin family can be subdivided into two groups: proteins that clearly accelerate *cis*/*trans* isomerization of phosphor-(Ser/Thr)-Pro moieties, as it has been demonstrated for human Pin1 (*h*Pin1) [4], yeast Ess1 [9] and some Pin1-type plant parvulins [10–12], and proteins that do not show any preference for phosphorylated substrates, such as *h*Par14 [13]. Human Pin1, like other Pin1-type PPIases, contains two domains that are important for the *in vivo* function of these proteins: an N-terminal WW domain and a C-terminal PPIase domain. The WW domain consists of 35- to 40-amino acid residues and acts as a protein–protein interaction module in many different proteins [14]. Depletion of *h*Pin1 in HeLa cells and depletion of its functional homolog Ess1 in yeast results in mitotic arrest, while overexpression causes G2 arrest [4]. Pin1 is mainly localized in the nucleus [4,15] and interacts specifically with proteins involved in cell cycle regulation [7]. In addition, Ess1 and Pin1

Abbreviations: FHA, forkhead-associated domain; NH-Np, 4-nitroanilide; PPIase, peptidyl-prolyl *cis*/*trans* isomerase; Par45^{PPIase}, residues 241–421 of *Tc*Par45

☆ The nucleotide sequence reported in this paper has been submitted to the GenBank™/EBI Data Bank with accession number(s) FJ409872.

* Corresponding author. INGEBI-CONICET, Vuelta de Obligado 2490, 2nd Floor, ADN1428, Buenos Aires, Argentina. Tel.: +54 11 4783 2871; fax: +54 11 4786 8578.
E-mail address: mtellez@dna.uba.ar (M.T. Téllez-Iñón).

0167-4889/$ – see front matter © 2010 Elsevier B.V. All rights reserved.
doi:10.1016/j.bbamcr.2010.05.006

have been shown to interact with both the C-terminal domain (CTD) of RNA polymerase II (Pol II) and other proteins that are important for RNA-Pol II transcription and regulation [16–19].

On the other hand, human Par14 lacks the N-terminal WW domain of *h*Pin1 and carries an unstructured N-terminal extension which is indispensable for its nuclear localization and binding to DNA [20,21]. Although *h*Par14 cannot rescue the lethal phenotype of Ess1 deletion, which is the only parvulin-type PPIase in yeast [11], Uchida and co-workers [22] proposed a compensating function for *h*Par14 upon *h*Pin1 inhibition or deletion in mammalian cells. In addition, *h*Par14 has been proposed as an *h*Pin1 complementing enzyme in cell cycle regulation and chromatin remodeling [21,22]. This parvulin displays a strong preference for peptide substrates containing an Arg side-chain preceding the Pro residue but not for phosphorylated Ser/Thr, as is the case of Pin1, and hence might also perform cellular regulatory functions different from those of Pin1 [13]. Recently, it has been reported that Par14 associates with multiple pre-ribosomal ribonucleoprotein (pre-rRNP) complexes formed at the various stages of mammalian ribosome biogenesis and that its knockdown suppresses cell growth [23].

The TriTryp kinetoplastids *Trypanosoma cruzi*, *Trypanosoma brucei* and *Leishmania major* are causative agents of different human diseases: Chagas' disease, sleeping sickness and leishmaniasis, respectively. We have previously reported the characterization of a Pin1-like PPIase named *Tc*Pin1 from *T. cruzi* [24]. Like all plant Pin1-like enzymes characterized so far, *Tc*Pin1 lacks the WW module. Additionally, in contrast to that observed with *h*Pin1-related proteins, *Tc*Pin1 is not nuclear. Aided by the availability of the completed genome sequence of *T. cruzi*, we have now identified a new member of the parvulin family of PPIases named *Tc*Par45, which is conserved in the TriTryp genome. Interestingly, a WW domain is not apparent in *Tc*Par45, but the presence of a forkhead-associated (FHA) domain in its place indicates that it may serve an equivalent function. To our knowledge, *Tc*Par45 is the first example of a FHA domain present in the same polypeptide with a PPIase domain.

To elucidate a possible role for *Tc*Par45 we studied herein its possible activity as a PPIase enzyme, its cellular localization and its substrate preferences. Additionally, we present an entire comparison of the substrate preference of all three parvulin-type PPIases, *Tc*Pin1, *Tc*Par14 and the novel *Tc*Par45. We found that *Tc*Par45 acts preferentially on substrates containing the basic Arg residue preceding Pro and does not complement yeast Ess1 temperature-sensitive mutants. These results are unexpected since the amino acid sequence of the catalytic core of the enzyme shows a high degree of similarity to Pin1-like PPIases, which are phosphorylation-dependent. Knockdown of the homologous protein in *T. brucei* (*Tb*Par45) by RNA interference (RNAi) caused a slow-growth phenotype, with a marginal increase in anomalous cells, thus indicating that it is required for normal cell proliferation.

This study provides new insights into the importance of a phosphorylation-independent parvulin-type PPIases.

2. Materials and methods

2.1. Sequence and phylogenetic analyses

Multiple protein alignments were based on the ClustalW algorithm using the NTI Vector Suite software (Informax Inc. Bethesda, MD, USA). A phylogenetic tree was built using the online service phylogeny.fr [25] ("A la carte" Mode), which implements the distance-based method Neighbor [26] for the construction of the phylogenetic tree and Treedyn to produce the image presented here.

2.2. Cell cultures

T. cruzi epimastigote, bloodstream trypomastigote and intracellular amastigote cells from the CL-Brener strain were cultured as previously described [24].

2.3. Cloning of *Tc*Par14 and *Tc*Par45 PPIases and their expression in *Escherichia coli*

The coding regions of the parvulins were amplified from genomic DNA by PCR using *Pfu* polymerase. PCR reaction conditions were as follows: initial denaturation cycle at 94 °C for 1 min, followed by 25 cycles of 94 °C for 1 min, 60 °C for 20 s, 72 °C for 1–2 min, and a final extension of 10 min at 72 °C. The primers for PCR cloning of the *TcPar14* gene were Par14F 5′-AAGGATCCGATGGGCAAGG AGAAGAA-3′ and Par14R 5′-ATCCTCGAGCTG TTTGTCCTCA ACCAA-3′ as sense and antisense primers respectively. The inserted restriction sites are underlined. The primers for PCR cloning of the region encoding the C-terminal end of the *TcPar45* gene were Par45F 5′-TTGGATCCAACCATCAACGCGAG G-3′ and Par45R 5′-ATAGTCGACCTACTCCGCGCGGTAAA-3′ as sense and antisense primers, respectively. The PCR product corresponding to the full-length gene sequence of *TcPar14* was inserted into the pET22b(+) (Novagen) vector by constructing unique *Bam*HI and *Xho*I sites at the 5′ and 3′ ends of the coding regions. The 546-bp band corresponding to the gene sequence encoding the C-terminal end of *Tc*Par45 (residues 241–421) was cloned into the *Bam*HI and *Sal*I restriction sites of the pET28a expression vector to generate the recombinant protein with an N-terminal histidine tag. The cloned PCR fragments were sequenced using single primer extension to confirm that no PCR-induced mutations had been introduced (Macrogen Inc.).

2.4. Recombinant protein expression

For expression of recombinant pET22/*Tc*Par14-His_6 and pET28/His_6-*Tc*Par45^{PPIase} (residues 241–421), the *E. coli* strain BL21-CodonPlus (DE3)-RIL was used. Cells were grown at 37 °C in LB medium to an $A_{600\ nm}$ of 0.7. Protein expression was induced by adding IPTG, to a final concentration of 0.5 mM and incubating for 5 h. Subsequently, the bacterial pellet from a 6×1 L culture was harvested and resuspended in lysis buffer containing 25 mM Tris/HCl buffer, pH 8.0, 300 mM NaCl, 5% glycerol, 5 mM $MgCl_2$, 10 mM imidazole and protease inhibitor cocktail (Roche), and lysed on a SLM Aminco French pressure cell. The extract was then clarified by ultracentrifugation at 50,000×*g* for 30 min and the supernatant was loaded on a nickel-nitrilotriacetic acid-agarose affinity resin previously equilibrated with the same buffer at 4 °C. Elution was carried out in a 50- to 300-mM imidazole gradient and fractions containing the enzymes were pooled and protein purity was analyzed on 15% (w/v) SDS-PAGE stained with Coomassie blue. Proteins were dialyzed against 10 mM HEPES pH 7.8, 1.5 mM $MgCl_2$, 150 mM KCl and 1.0 mM DTT and concentrated by using Centricon (Millipore) tubes. Finally, samples were applied to a Superdex 75 column (Amersham Pharmacia) equilibrated in the same buffer. Fractions were collected, analyzed by SDS-PAGE and the resulting fractions containing the enzymes were used for determinations of PPIase activity.

2.5. Antibody generation and purification

Antibodies to *Tc*Par14 and *Tc*Par45 were generated in rabbit with His-*Tc*Par14 and His-*Tc*Par45^{PPIase} fusion proteins as antigens, respectively. The immunization followed a standard protocol. For affinity purification, His-*Tc*Par14 and His-*Tc*Par45^{PPIase} fusion proteins were independently coupled to Affi-Gel 10 (Bio-Rad) according to the manufacturer's protocol. Complete serum was incubated with the column at 4 °C and specific antibodies were eluted using 0.1 M glycine pH 2.5. Samples were neutralized and protein concentration was assayed. The antibody to *Tc*Pin1 has been previously described [24].

2.6. PPIase: peptidyl-prolyl *cis*/*trans* isomerase activity assay

PPIase activity was assayed basically as previously described [24], using the protease-free PPIase assay according to Janowski et al. [27].

PPIase activities were measured at 10 °C in 35 mM sodium HEPES buffer, pH 7.8, with a Hewlett-Packard 8453A UV/Vis spectrophotometer. A 30-mM stock solution of the substrates (Bachem) in 0.5 M LiCl/TFE (2,2,2-Trifluoroethanol anhydrous) was freshly prepared before the measurements. Prior to every measurement, all components except the substrate were preincubated for 300 s at 10 °C under vigorous stirring. Each measurement was started after substrate addition (60 μM final substrate concentration) and the *cis*/*trans* isomerization kinetics of the substrate was followed at 330 nm.

2.7. Yeast complementation analysis

The yeast complementation assay was performed as previously described [24]. Briefly, the *T. cruzi* parvulins *Tc*Pin1, *Tc*Pin1^{R20A}, *Tc*Par14 and *Tc*Par45 full-length were subcloned into the yeast expression vector pJK305-TPI, which allows constitutive expression of the protein. Temperature-sensitive yeast cells (MATa ess1H164R integrated into the W303 1A yeast strain) [28] were grown overnight in YPAD (yeast extract/peptone/adenine/dextrose) medium at 30 °C and were then transformed with the different constructions via electroporation. Gene expression in the stably transformed YGD-ts22W strains was controlled by Western blot analysis of the cell lysates from cultures grown at permissive temperature (30 °C) using the specific antibodies. For the complementation analysis, cells of the respective strain selected in the appropriate medium at permissive temperature were resuspended in 10 mM Tris/HCl buffer, pH 7.5, 1 mM EDTA and the optical density adjusted to $A_{600} = 0.5$. A 10-fold series dilution was performed and 5 μl of each dilution was spotted onto the plates. In order to test for functional complementation, the cells were incubated at both permissive (30 °C) and non-permissive (37 °C) temperatures. Cells carrying both the pJK305-TPI vector without the insert and human Pin1 were used as controls.

2.8. Immunofluorescence microscopy

T. cruzi epimastigote and *T. brucei* procyclic cells were washed with PBS, attached to 0.1% poly-L-lysine-coated glass slides and fixed with 4% formaldehyde in PBS for 20 min, and then permeabilized with 0.1% Triton X-100 in PBS for 5 min at room temperature. Par45 was detected by incubating cells with the rabbit affinity-purified antibody diluted to 1:400 in PBS. The Alexa Fluor 546-conjugated goat anti-rabbit antibody (Molecular Probes, 1:500) was used as the secondary antibody. The flagellum was revealed by anti-paraflagellar rod (anti-PFR) monoclonal antibody (1:2; hybridoma supernatant provided by Dr. S. Schenkman), followed by an Alexa Fluor 488-conjugated anti-mouse secondary antibody (Molecular Probes, 1:500). V5-tagged Par45 was detected with the mouse monoclonal antibody (Invitrogen; 1:200) and the Alexa Fluor 546-conjugated goat anti-mouse antibody (Molecular Probes, 1:500). Nuclear and mitochondrial DNA was stained with DAPI. All slides were mounted in Vectashield (Vector) in the presence of 10 μg of DAPI per ml. Serial images (0.2-μm Z-increment) were collected using a 100× objective 1.35 NA using the Cell M software in a motorized Olympus IX81 microscope. Images were processed by blind deconvolution using Autoquant X 2.1. Alternatively, images were taken using an Olympus BX41 light and fluorescence microscope with an Olympus DP71 digital camera and capture software (Olympus America, Inc, Center Valley, PA) and exported as TIFF files for assembly in Adobe Photoshop CS3 (Adobe System, Inc., San Jose, CA).

2.9. Parasite transfection and RNAi experiments

For transfection of the procyclic *T. brucei* form, 10^7 cells were washed once in 5 ml of cytomix [29] and resuspended in 0.5 ml of cytomix containing 10 μg of *Not*I linearized plasmid so that it could target the rDNA spacer region [30]. Transfections were carried out in 4-mm cuvettes using a Bio-Rad electroporator with peak discharge at 1.6 kV and 25 μF of capacitance. Immediately after transfection, cells were transferred into 10 ml of SDM-79 supplemented with G418 and hygromycin. After 1 day, selection was applied by culturing the cells in the presence of 2.5 μg/ml phleomycin for 2 weeks to form stable lines. RNAi experiments used the procyclic *T. brucei* 29-13 strain which harbors genes for T7 RNA polymerase and the tetracycline repressor [31]. Procyclic parasites were cultured at 28 °C in SDM-79 medium containing 10% fetal bovine serum (FBS, PAA Laboratories GmbH). Media were supplemented with appropriate selection agents (hygromycin, 50 μg/ml; G418, 15 μg/ml; phleomycin, 2.5 μg/ml; blasticidin, 10 μg/ml). For RNAi, *T. brucei* 29-13 expressing V5-tagged Par45 was transfected with the pZJM vector [30], whose insert was a PCR-amplified fragment of the *TbPar45* gene (encoding amino acid residues 21–189; accession number Q57XM6). After drug selection, the transfected cells were cloned by limiting dilution, generating independent Par45RNAi cell lines. To evaluate the effects of RNAi on cell proliferation, cells cultured in SDM-79 in the absence (−tet) or presence (+tet) of tetracycline were counted daily and cumulative growth curves for each clone were plotted on a logarithmic scale. *In situ* tagged *TbPar45* ORF was obtained by amplifying ~300 bp regions in the 5′UTR of the gene and the 5′ region of the ORF. The primers UTRPar45F 5′-TACCGCGG CATTTTCGATGCAC-3′ and UTRPar45R 5′-CCTCTAGATTCCTC-CACCCCTCGC-3′ were used to amplify the 5′UTR region, whereas the primers ORFPar45F 5′-CGCTCGAGATGGTTA CCTCTACTGC-3′ and ORF-Par45R 5′-ATGGGCCCGTCGCCTCTT CT-3′ were used to amplify the 5′ region of the ORF. The fragments were cloned both upstream and downstream of the BLA/V5 cassette [32] to yield the plasmid pBLA/V5-Par45. This plasmid was digested with *Apa*I/*Not*I and transfected into procyclic 29-13 *T. brucei*. For detection of V5-tagged proteins, a 1/1000 dilution of the anti-V5 antibody (Invitrogen) was used.

2.10. Northern blot

Total RNA was obtained using TRIzol reagent (Invitrogen) according to the manufacturer's instructions and Northern blotted as previously described [24]. Probes for *Tb*Pin1 (AAX69357), *Tb*Par14 (Tb927.3.3100) and *Tb*Par45 (Q57XM6) were full-length open reading frames. The probes were radiolabeled with [α-^{32}P] dCTP (10^9 cpm pmol^{-1}, NEN) using the Prime-a-Gene Labeling System (Promega). Quantification was performed using a phosphorimager Storm 820 (Amersham Pharmacia Biotech) and ImageQuant software. Ribosomal RNA was used to measure loading. Experiments were performed at least twice and representative results from individual experiments are shown.

2.11. Other procedures

A Western blot was performed as described previously [24]. The mouse monoclonal anti-β tubulin was purchased from Amersham Life Science. Epimastigote cells from the Tulahuen strain were synchronized as described previously [33]. Samples were analyzed using a Becton Dickinson ExCalibur Flow Cytometer (Becton Dickinson, San Jose, CA) and graphed using WinMid 2.9 software.

3. Results

3.1. TcPar45 is a new member of the parvulin family of PPIases in trypanosomes

Two eukaryotic parvulin-related PPIases, *h*Pin1 [4] and *h*Par14 [13], have been previously identified in humans. We have previously reported two parvulins in *T. cruzi*, named *Tc*Pin1 and *Tc*Par14, as molecular homologs of the human Pin1 and Par14 PPIases, respectively [24]. We used human parvulin protein sequences to search for additional putative PPIases in the genome of *T. cruzi*. Both queries gave high amino acid identity scores over the parvulin catalytic domain (35.4% and 17.7%

respectively) for a protein encoded by a gene annotated as a hypothetical protein in *GeneDB* (http://www.genedb.org/) data base (Tc00.10470 53509207.130). We have named this protein *Tc*Par45 (for *T. cruzi* Parvulin) according to Fischer [34]. *Tc*Par45 encodes a 421-amino-acid protein, which has a predicted size of 45.4 *k*Da. It encodes a parvulin domain highly similar to that of Pin1-like PPIases and an N-terminal FHA domain usually found in proteins involved in nuclear signaling [35]. An alignment of the PPIase domain of the Par45 sequence with homologs of *h*Pin1 from selected organisms is shown in Fig. 1, panel A. A search in the TriTryp genome databases revealed that putative Par45-type PPIases homologs are present in all trypanosomatids, with a high degree of identity. The *Tc*Par45 catalytic domain (residues 309–421) shares a high degree of homology with the phosphorylation-dependent eukaryotic Pin1-type. The degree of homology to the PPIase domains of other Pin1-

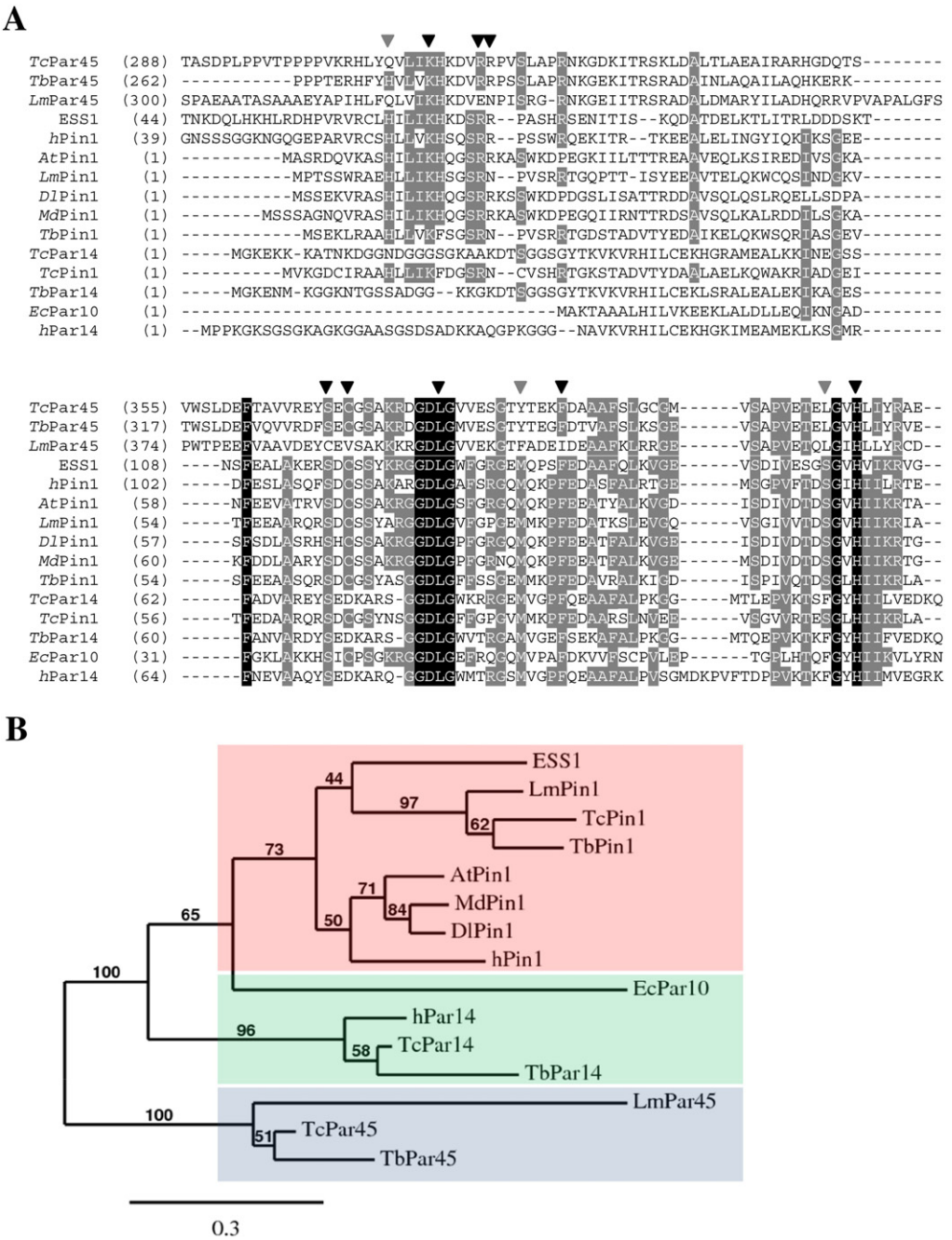

Fig. 1. Multiple sequence alignment of Par45-related proteins (Panel A). Identical (*black*) or conservatively substituted (*gray*) residues in at least 50% of the sequences are highlighted. The residues shown by both the crystal structure of human Pin1 [5] and site-directed mutagenesis experiments [5,36,37] to be within the active site of the PPIase moiety are indicated by *triangles*. The residues believed to be important for PPIase activity are highlighted in black triangles when conserved between *Tc*Par45 and *h*Pin1; otherwise in gray. The sequences were aligned over their entire length using ClustalW. Phylogenetic tree for the parvulin proteins (Panel B). The phylogenetic tree was built using the distance-based method Neighbor [26] (1000 bootstrap replicates) based on a multiple sequence alignment generated using ClustalW. The tree is drawn to scale using Treedyn. Different background colors correspond to different parvulin subfamilies: phosphorylation-dependent PPIases (*red*) [10–12,24,50,51], Par45-related (*blue*, this work), and a group of proteins with varying substrate specificity (*green*) [13,52]. Sequences included are as follows: *Tc*Par45 is from *T. cruzi* (FJ409872), *Tb*Par45 from *T. brucei* (Q57XM6), Ess1 from *Saccharomyces cerevisiae* (CAA59961) [50], *h*Pin1 and *h*Par14 from humans (AAC50492 and AB009690, respectively) [13,51], *AtPin1* from *Arabidopsis thaliana* (AAD20122) [10], *DlPin1* from *Digitalis lanata* (AJ133755) [11], *Md*Pin1 from *Malus domestica* [12], *Tb*Pin1 and *Tb*Par14 from *T. brucei* (AAX69357 and Tb927.3.3100, respectively), *Tc*Pin1 and *Tc*Par14 from *T. cruzi* (DQ303420 and DQ420359, respectively) [24], *Lm*Pin1 and *Lm*Par45 from *L. major* (CAJ07069 and LmjF22.0530, respectively) and *Ec*Par10 from *E. coli* (S48658) [52].

like enzymes were found to be 42% with Ess1 from *Saccharomyces cerevisiae*, 33% with *At*Pin1 and 27% with *Tc*Pin1 from *T. cruzi*. There is less sequence homology with other parvulins with a rather unspecific substrate recognition pattern, such as *Ec*Par10 from *E. coli,* which has 19% identity to the PPIase domain of *Tc*Par45.

Residues essential for catalysis have been proposed for Pin1-like parvulins based on a complex structure of human Pin1 with an Ala-Pro dipeptide and a sulphate bound to the active site [5] in line with site-directed mutagenesis experiments [5,36,37]. The phosphate binding site, which is defined by Lys63, Arg68, and Arg69 and thought to be the catalytic loop in *h*Pin1, is conserved among the Pin1-type parvulins and the novel *Tc*Par45 (Fig. 1, panel A). In the *Tc*Par45 enzyme, the specific sequence features exist as Lys312, Arg317, and Arg318. Remarkably, the PPIase protein sequence of *Tc*Par45 is closer to that of human Pin1 [5,36,37] and shows a better conservation of critical residues than that of *h*Par14 [38,39] (Fig. 1, panel A). The phylogenetic relationship between the 15 parvulin sequences used in the multiple alignment is shown in Fig. 1, panel B. This phylogeny, based on the PPIase domain sequences of parvulins, supports the existence of a novel parvulin family with unique features.

Proteins sharing similar domain architecture are present only in a few other eukaryotic organisms. A search in all publicly available genome databases revealed that putative Par45 orthologs are present in the slime mold *Dictyostelium discoideum* and in the unicellular green alga *Chlamydomonas reinhardtii*. In addition to protozoa and algae, we detected several divergent proteins containing the single module protein–protein interaction FHA domain, showing similarity to that of Par45. The protein–protein interaction domain of *Tc*Par45 showed 38% amino acid sequence identity to the FHA domain of NIPP1 (nuclear inhibitor of protein phosphatase 1). However, this divergent protein does not contain a PPIase domain.

These characteristics indicate that *Tc*Par45 is an atypical member of the parvulin family, distinct from those previously characterized in mammals, yeast and plants.

3.2. Detection of the native protein in parasite extracts

The expression pattern of *T. cruzi* Par45 protein was studied in all life cycle stages of the parasite using serum affinity-purified antibodies obtained against the recombinant *Tc*Par45^{PPIase} protein. As shown in Fig. 2A, the anti-*Tc*Par45 antiserum recognizes a 45-*k*Da protein in total cell extracts in all three life cycle stages of the parasite. On the other hand, the pre-immune serum did not react with parasite protein lysates. Next, we asked whether Par45 protein levels fluctuated during the cell cycle. To address this question, epimastigote cells were hydroxyurea (HU) synchronized [33]. After removal of the HU, the cells underwent a short lag period and then proceeded synchronously through the cell cycle. At different times after the release from the block, cells were harvested and analyzed by flow cytometry or lysed and analyzed for protein expression by immunoblotting. Analysis of the DNA content indicated that the cells progressed synchronously through different phases of the cell cycle (Fig. 2B, *left*). Nonetheless, total Par45 levels did not change significantly during the cell cycle (Fig. 2B, *right*).

3.3. TcPar45 is a functional PPIase in vitro

Attempts to produce Par45 as a full-length recombinant protein in *E. coli* were unsuccessful. The overexpression of Par45 inhibited the bacterial growth rapidly after inducing parvulin expression. This phenomenon was most likely caused by its FHA domain, given that the overexpression of this isolated domain causes the same phenotype (data not shown). Therefore, the function of *Tc*Par45 as a PPIase was tested by expressing a C-terminal fragment containing the catalytic domain of the enzyme. For identification, the molecular mass of 6xHis-*Tc*Par45^{PPIase} was determined at 22,937 Da by matrix-assisted laser desorption time-of-flight mass spectrometry (data not shown). The PPIase activity of the purified C-terminal fragment of *Tc*Par45 was determined by using the protease-free assay. Under these conditions, the substrate specificity of the isolated catalytic domain of *Tc*Par45 toward the substrate succinyl-Ala-Arg-Pro-Phe-NH-Np resulted in a k_{cat}/K_M value of 97.1 ($\pm$1.7)$\times 10^3$ /M/s, whereas the isomerase activity for substrates containing different Pro bonds exhibited lower activity (Table 1). The relative specificity values for various substrates showed a pattern similar to that of the human and trypanosome Par14, with a preference for a substrate with the basic Arg residue preceding proline. For instance, the substrate Suc-Ala-Arg-Pro-Phe-NH-Np was interconverted with a specificity constant k_{cat}/K_M of 194 /mM/s by *Tc*Par14. This is about 50-fold higher than the respective value of k_{cat}/K_M for human Par14 [13].

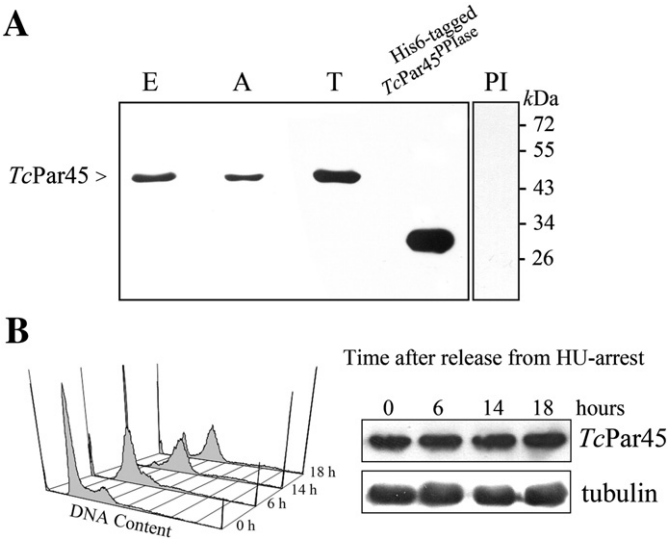

Fig. 2. (A) Western blot analysis of *Tc*Par45. Immunoblot analysis of whole-cell extracts from epimastigote (**E**), amastigote (**A**) and trypomastigote (**T**) form cells (60 μg each) and the recombinant His-tagged *Tc*Par45^{PPIase} protein purified from *E. coli* (200 ng) as control, resolved by SDS-PAGE (10% gels), electrotransferred onto Hybond C membranes, and revealed with affinity-purified anti-*Tc*Par45 antibody (1:1000; *left*). The position of 45 *k*Da *Tc*Par45 is indicated. Pre-immune (PI) serum was used as control (1:1000; *right*). (B) *Tc*Par45 levels are constant during the cell cycle. Epimastigote cells were harvested at the indicated times after HU removal and aliquots were subjected to flow cytometric analysis to determine the cell cycle status and the remaining cells were analyzed for protein expression by immunoblotting. (*left*) Flow cytometric analysis of the DNA content. Cells at 0 (G1), 6 (S), 14 (G2/M) and 18 hours after release from HU are shown. (*right*) The same amounts of total proteins (60 μg) were separated on an SDS-containing gel, transferred to a membrane and probed with anti-*Tc*Par45 (1:1000; *upper*) and anti-β tubulin antibodies (1:5000; *bottom*).

In contrast to Pin1-like PPIases, but similarly to *Tc*Par14, *Tc*Par45^{PPIase} does not accelerate the *cis* to *trans* interconversion of substrates with negatively charged Glu amino acid residues preceding Pro bonds (Table 1), despite the high sequence identity of the PPIase active sites (Fig. 1, panel A). These results indicate that *Tc*Par45 is active as a PPIase enzyme and suggest that this parvulin is more specific towards substrates containing a basic Arg residue preceding proline.

3.4. Yeast complementation analysis

We have previously demonstrated that *Tc*Pin1, similarly to Pin1-like PPIases, is able to complement the otherwise lethal Ess1 loss in *S. cerevisiae* [11,12,24]. Given the homology of the PPIase catalytic domains of *Tc*Par45, *Tc*Pin1 and human Pin1 we decided to evaluate whether Par45 is able to replace Pin1/Ess1 functions in yeast. The strain used grows normally at 30 °C but arrests at G2/M transition after two to three generations at 37 °C (restrictive temperature) [28]. The complete parvulin genes of *T. cruzi* were subcloned in the *S.*

Table 1
Substrate specificity constants (k_{cat}/K_M) of TcPar45^{PPIase} and comparison of the specificity pattern to related *T. cruzi* PPIases.

Xaa	*Tc*Par45^{PPIase}		*Tc*Par14	*Tc*Pin1
	k_{cat}/K_M ($\times 10^3$ /M/s)	Relative activity (%)	Relative activity (%)	Relative activity (%)
Arg	97.1 (± 1.7)	100	100	100
Glu	7.4 (± 0.8)	7.6	0.9	3202
Phe	4.2 (± 0.1)	4.3	0.6	26.6
Leu	25.9 (± 2.1)	26.7	2.4	141.1
Ala	6.7 (± 0.3)	6.9	1.0	124.2

Substrates were of the type Suc-Ala-Xaa-Pro-Phe-NH-Np, where Xaa stands for a variable amino acyl residue. The relative activities were normalized to the value of k_{cat}/K_M of the substrate Suc-Ala-Arg-Pro-Phe-NH-Np. The values for that substrate were estimated as follows: *T. cruzi* Par14 $k_{cat}/K_M = 194$ /mM/s and *Tc*Pin1 $k_{cat}/K_M = 12.4$ /mM/s. The values concerning *Tc*Pin1 were calculated from data of [24] and from this work. PPIase measurements were performed in a protease-free assay as described under Materials and methods.

cerevisiae expression vector pJK305-TPI and transformed in the budding yeast Ess1^{ts}. As it has been previously described [24], after selection on Leu-deficient minimal medium plates, only colonies containing the *TcPin1* gene grew at the restrictive temperature (Fig. 3A). In contrast, neither *Tc*Par14 nor *Tc*Par45 abolished the temperature sensitivity of the yeast cells. Moreover, a point-mutation variant of *Tc*Pin1 (*Tc*Pin1^{Arg20Ala}), engineered to make the coordination of the phosphate group of the substrate impossible, was not able to rescue the lethal phenotype (Fig. 3A). In the same set of experiments, human Pin1 was used as a positive control. Immunoblotting analysis of lysates from YGD-ts22W cells transformed with the different constructs using specific antibodies showed that all proteins were expressed at comparable levels (Fig. 3B). Intriguingly, we observed that *Tc*Par45 displays an apparently higher molecular weight than the expected one, probably due to post-translational modifications occurring in the yeast. Failures of transformed mutant cells to grow at 37 °C are in agreement with the kinetics parameters observed in the *in vitro* PPIase assay.

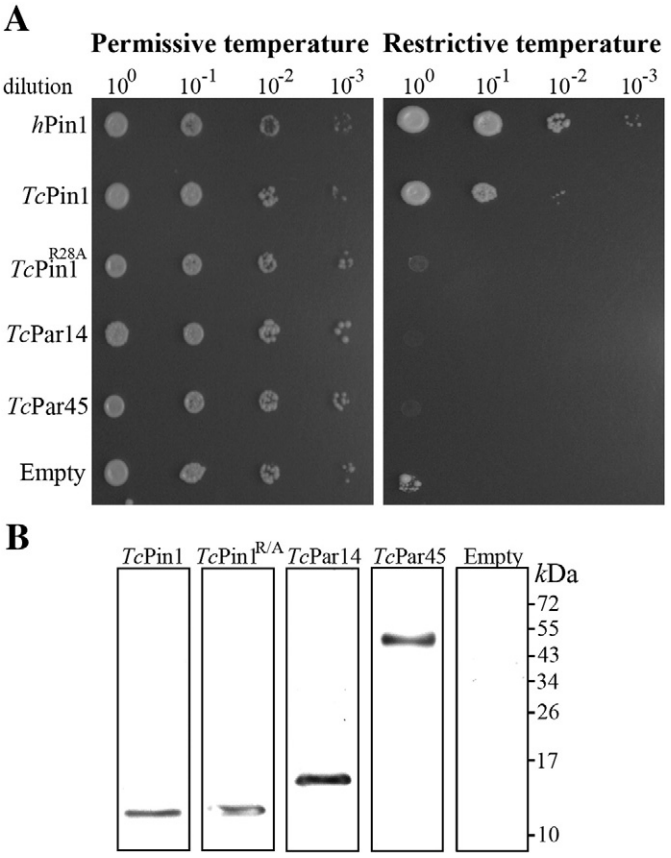

Fig. 3. Only *Tc*Pin1 can suppress the temperature-sensitive phenotype of the yeast strain YGD-ts22W under non-permissive temperature. (A) The strain was transformed with the yeast expression vector pJK305-TPI containing the coding sequence of the *T. cruzi* parvulins *Tc*Pin1, *Tc*Pin1^{R20A}, *Tc*Par14 and *Tc*Par45. Data were obtained after 2–4 days of incubation at permissive (30 °C) or non-permissive temperatures (37 °C). From left to right, 10-fold dilutions of the initial cell suspension were plated into synthetic selective media (without leucine). Cells expressing either *h*Pin1 (*upper*) or the empty vector (*bottom*) were used as positive and negative controls respectively. (B) Similar expression of transgenes in yeast cells. YGD-ts22W strains stably transformed with various *T. cruzi* parvulin constructs were subjected to immunoblotting analysis using specific affinity-purified antibodies (1:500 dilutions) obtained as described under Materials and methods. Cells transfected with the empty vector were separated by electrophoresis and revealed using anti-*Tc*Par45 antibody (1:500 dilution).

3.5. TcPar45 is a nuclear protein

A large number of the characterized FHA-containing proteins have been reported to be localized in the nucleus [35]. In agreement with these observations, Par45 has a nuclear localization, although it lacks any other canonical nuclear-localization signal. To determine the subcellular localization of *T. cruzi* Par45, we used different experimental approaches. Indirect immunofluorescence assays of epimastigotes indicated that *Tc*Par45 is highly concentrated within the nuclei but also revealed some degree of cytoplasmic localization (Fig. 4A). No signal was detected when using the pre-immune serum (Fig. 4B) or the secondary antibody alone (results not shown). In addition, examination of epimastigotes expressing GFP fused to the C-terminal domain of *Tc*Par45 revealed that the fluorescence was mainly restricted to the nuclei (data not shown). Interestingly, using immunofluorescence with anti-*Tc*Par45 antibody, we found that *Tb*Par45 localization in the procyclic form of *T. brucei* closely resembles that of the *T. cruzi* parvulin protein (Supplemental data S1). In addition, to detect *Tb*Par45 in procyclic form we used cell lines in which a sequence encoding a V5 tag [32] had been introduced at the 5′ end of the gene by homologous recombination. In these cells, the same nuclear pattern was observed (Supplemental data S2). Taken together, these results indicate that Par45 is mainly concentrated in the nuclei of both *T. cruzi* and *T. brucei* parasites.

3.6. Silencing of TbPar45 expression causes a slow-growth phenotype

Gene-specific silencing by RNA interference (RNAi) is a valuable tool for the analysis of gene function in the protozoan parasite *T. brucei* [40]. Given that null mutants are difficult to obtain in *T. cruzi* and that RNAi has failed to function in this organism [41], we decided to explore the Par45 enzyme function in the procyclic form of the RNAi-positive protozoa, *T. brucei*. To investigate whether *Tb*Par45 depletion affected cell proliferation, an inducible RNAi cell line expressing V5-tagged Par45 was generated using the procyclic Lister 427 29-13 strain. Following initiation of RNAi, the cells were re-seeded every 24 h. The Northern blot analysis in Fig. 5 panel B shows that in RNAi-induced cells the level of Par45 mRNA was reduced by 63% on day 4. This analysis also showed that the *Tb*Pin1 or *Tb*Par14 mRNA abundance was not affected in Par45RNAi cells (Fig. 5, panel B). V5-tagged *Tb*Par45 protein levels in induced cultures reached a minimum of roughly 20–40% of that in non-induced cells after 2 days (Fig. 5, panel A). We next evaluated the effect of RNAi on cell growth. RNAi-induced cells grew normally for 3–4 days and then continued at a lower rate, indicating that Par45 is required for maximum growth rate (Fig. 5, panel C). Probably, the remaining levels are responsible for the delayed onset of the growth phenotype. The effect on cell division and kinetoplast segregation was monitored by staining of the nuclear (N) and mitochondrial DNA (kinetoplast [K]) with DAPI and visualization by fluorescent microscopy (Fig. 5, panel D). The cells in G1 and S phases seem to have one nucleus and one kinetoplast (1N1K). Since K division precedes nuclear division, cells in the G2/M

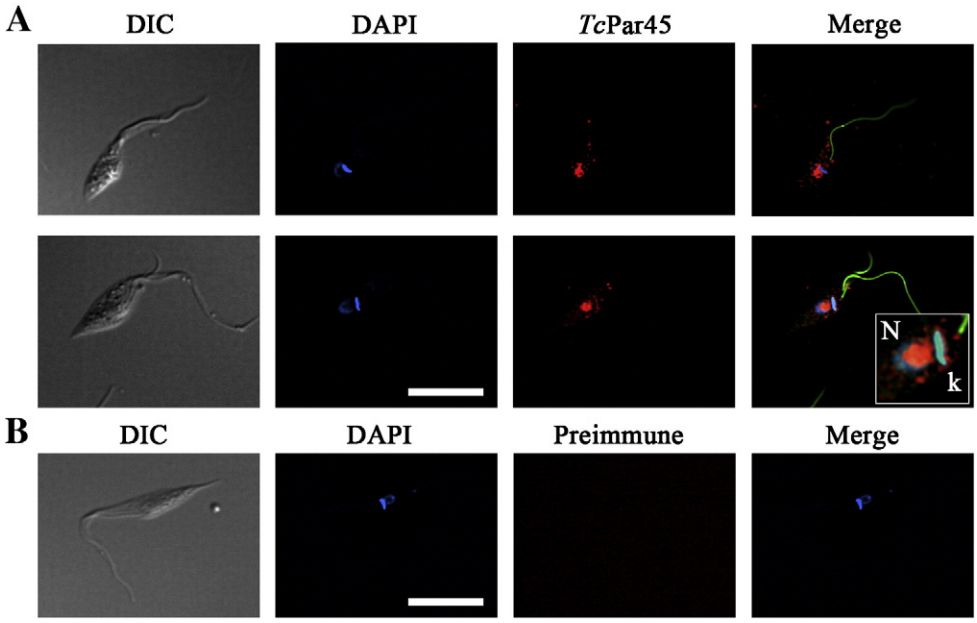

Fig. 4. Localization of *Tc*Par45. (Panel A) Epimastigote cells were fixed and the endogenous Par45 protein was detected with anti-*Tc*Par45 (1:200) and an Alexa 546-conjugated anti-rabbit secondary antibody. Flagella were revealed with an anti-paraflagellar rod (anti-PFR, 1:2 dilution) mAb, followed by an Alexa 488-conjugated anti-mouse secondary antibody. Phase contrast, DAPI staining and *Tc*Par45 signals are indicated. The nucleus (N) and kinetoplast (k) were stained with DAPI. No significant background staining was observed when preimmune serum was used as a control (Panel B). The inserted box represents 2.5× zoom of the merge image. The images show one deconvolved Z-section using Autoquant X 2.1 software. Bar, 10 μm.

phase have one nucleus and two kinetoplasts (1N2K), and cells undergoing cytokinesis have two nuclei and two kinetoplasts (2N2K). In the control Par45 cell line (non-induced cells), 87% of the cells were found to have a normal-sized single nucleus and a single kinetoplast (1N1K); the rest of the cells (13%) were mainly either 1N2K or 2N2K. In induced cells, there was however, a marginal increase in the

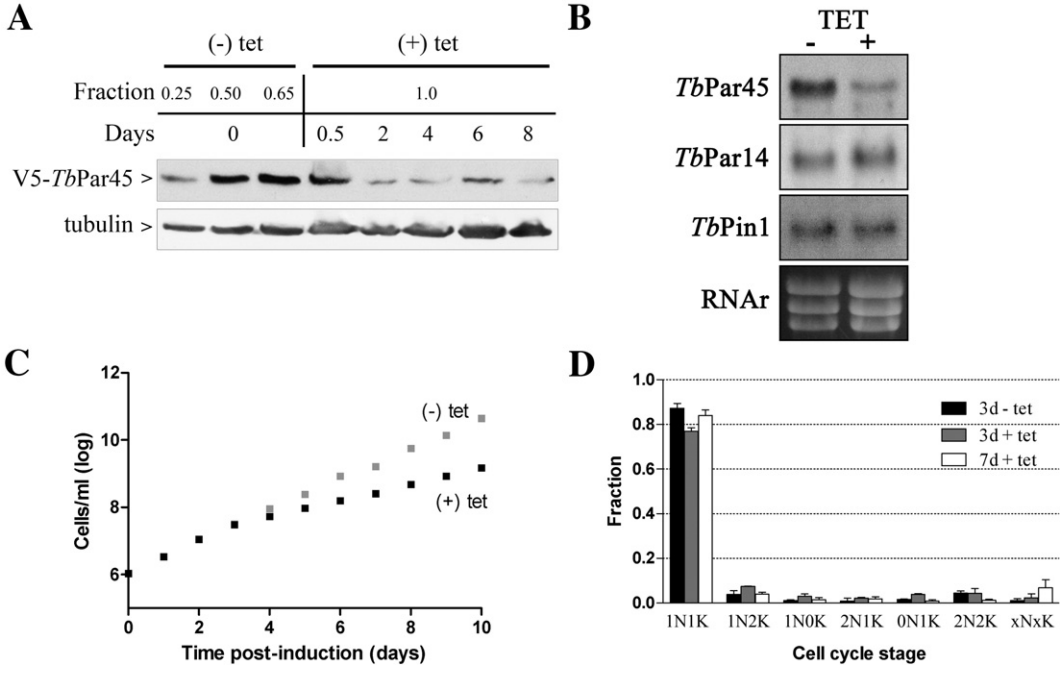

Fig. 5. Effects of RNAi on *Tb*Par45 in procyclic cells. *Tb*Par45-RNAi cells were grown in the presence or absence of tetracycline and samples were taken for immunoblotting and counting. The cultures were re-seeded at 10^6 cells/ml with fresh tetracycline every 24 h. (Panel A) Summary of quantitative immunoblotting of *Tb*Par45 during RNAi induction. A time-course representative immunoblot of cell lysates using anti-V5 antibody (1:1000) is shown. The lysate from the non-induced sample was serially diluted and lanes with 25–65% of the original amount are shown. An antibody recognizing β-tubulin (1:5000) was used as the load control. (Panel B) Northern blot showing specific effect of RNAi on Par45 mRNA level. A Northern blot was made with 30 μg of total RNA (3 days after tetracycline addition for RNAi cells), probed with ^{32}P-labeled *Tb*Par45 and then reprobed with *Tb*Pin1 and *Tb*Par14 and the resulting signals analyzed by PhosphorImager. The RNAr was used as loading control. (Panel C) Representative growth curves of *Tb*Par45 RNAi cells in the presence or absence of tetracycline. (Panel D) Silencing of *Tb*Par45 expression increases the number of aberrant cells. Quantification of the cell cycle stages of the *Tb*Par45 RNAi cells on the 3rd and 7th day time points. On the 7th day time point there is a marginal accumulation of xNxK cells. Data were compiled from three independent experiments (n>1000 cells/time point), normalized relative to total cell number, and expressed as mean ± SE.

number of aberrant xNxK cells. Similar results were observed in induced RNAi cell lines expressing endogenous (non-tagged) *Tb*Par45 (data not shown).

4. Discussion

In this study, we identified and characterized a new member of the parvulin-type PPIase subfamily, Par45, which is required for normal cell proliferation in trypanosomes. Par45 represents the first molecule characterized that, in addition to a parvulin-like PPIase domain, contains a conserved FHA protein–protein interaction domain. As most characterized Pin1-like enzymes in eukaryotic organisms, Par45 exhibits an N-terminal extension beyond the conserved PPIase domain extending for approximately 300 amino acids. Interestingly, in most metazoans, the phospho-dependence of the substrate recognition of Pin1-like PPIases requires a specialized WW domain at this position [42,43]. However, in Par45, a WW domain is not evident, but the presence of an FHA domain in its place could indicate that it may serve an equivalent function. This domain organization, including a PPIase and FHA, is found in some eukaryotic organisms such as the green alga *C. reinhardtii*, the slime mold *D. discoideum* and the trypanosomatids *T. brucei* and *L. major*, with potential orthologs not present in the existing genome databases of prokaryotes and higher eukaryotes such as plants and animals. The parvulin catalytic core of *Tc*Par45 displays striking similarity to the Pin1-type subfamily of the parvulins. For example, *Tc*Par45 shares 35.4% identity with the PPIase domain of *h*Pin1 and only 17.7% sequence identity with *h*Par14, the latter of which does not exhibit the phosphorylation-dependent substrate specificity (Fig. 1, panel A).

Attempts to express soluble *Tc*Par45 in *E. coli* under a variety of conditions were unsuccessful, precluding a complete biochemical study. Because of this, the determination of the PPIase activity of *T. cruzi* Par45 was performed using the recombinant catalytic PPIase fragment of Par45. It is expected that the kinetics parameters using the isolated catalytic domain of Par45 is present for the full-length PPIase. Using the substrate Suc-Ala-Arg-Pro-Phe-NH-Np, the specificity constant observed in the PPIase assay for *Tc*Par45^{PPIase} was about three orders of magnitude (about 2000-fold) lower than the respective value of k_{cat}/K_M for *T. cruzi* Par14 and about 40-fold less active than human Par14 [13]. A comparison of the relative values of the specificity constants for various substrates followed a pattern of *T. cruzi* Par14 with a preference for a substrate with the basic Arg residue preceding prolyl bonds (Table 1). Interestingly, based on the residues present in the Par45 sequence, and the presence of the basic triad composed of Lys312, Arg317, and Arg318, which forms the recognition site for the phosphate group of Pin1 substrates [5,36,37], Par45 is expected to exhibit a preference for acidic substrates, similar to that observed for *h*Pin1 and *Tc*Pin1. In this context, Par45 is a curious example that demonstrates the impossibility to ascribe substrate specificity based solely on sequence similarity. As it has been previously shown, although pSer or pThr-binding activity of the Pin1 WW domain is required for the protein function *in vivo*, the WW domain has no influence on the substrate specificity [42]. In addition, the low extent of the specificity constant of Par45^{PPIase} of 97.1 /M/s for the most favorable substrate may indicate that the reminiscent of the natural binding partner of this parvulin has not yet been found among the peptides assayed.

An excellent criterion for assigning parvulins to the Pin1-like subgroup is the ability to replace Pin1/Ess1 functions in yeast. Indeed, it has been shown that the PPIase domain of *h*Pin1 is sufficient for rescuing the temperature-induced lethal phenotype in budding yeast [8]. As we have previously verified, *Tc*Pin1 is able to complement the otherwise lethal Ess1 loss in *S. cerevisiae* [24]. Failure of *Tc*Par14 and *Tc*Par45 to rescue the lethal phenotype (Fig. 3) correlates with the kinetics parameters observed in the *in vitro* PPIase assay (Table 1).

The Par45 cellular localization is consistent with that of most FHA-containing proteins described [35]. Two methods designed to determine the cellular localization, the expression of the protein in fusion with GFP and the indirect immunofluorescence analysis, using the antibody generated against the recombinant fragment Par45^{PPIase}, indicated the same cellular distribution in both *T. cruzi* epimastigote cells and *T. brucei* procyclic form (Fig. 4 and Supplemental data S1 and S2). In epimastigote cells, Par45 localized predominantly within nuclei. Remarkably, the same subcellular localization was observed when endogenous *Tb*Par45 was V5-tagged in the procyclic-form cell line 29-13 of *T. brucei* (Supplemental data S2), suggesting that the localization of this modified version of the protein is not altered. Interestingly, *h*Pin1 has been localized almost exclusively in the cell nucleus and concentrated at discrete structures [15,44].

While it was possible to obtain low levels of GFP tagged-Par45 expressed in epimastigote forms of *T. cruzi*, overexpression of the molecule using the pTREX vector [45] could not be achieved (data not shown), thus suggesting that high levels of Par45 are toxic for parasite survival. Antibodies raised against *Tc*Par45 showed that the PPIase enzyme was present in all three stages of the parasite and that Par45 protein levels, as previously demonstrated for *h*Pin1 [7], is constant during the cell cycle (Fig. 2, panel B).

We here described the results of the downregulation of Par45 by RNAi in the procyclic form of *T. brucei*. The high degree of conservation between the Par45 proteins from *T. cruzi* and *T. brucei* (57.5% sequence identity, Fig. 1, panel A), and the fact that both proteins display a similar subcellular localization (Fig. 4 and supplemental data), allow us to infer a similar function in both parasites. In this study, loss of *Tb*Par45 in the procyclic form produced a mild growth defect and a slight increase in the number of abnormal xKxN cells (Fig. 5, panels A–D). Since immunoblotting showed that there was still approximately 20–40% of wild-type *Tb*Par45 levels present in the RNAi cells, it could be that this is sufficient to maintain cell growth. Actually, in budding yeast, vanishingly low levels of Ess1 PPIase activity are sufficient to support cell growth [46]. Taken together, these results suggest that Par45 might be involved in the control of cell cycle progression, as shown for Ess1 in yeast and for its counterpart Pin1 in HeLa cells [4]. However, the fact that *Tc*Par45 levels are constant in *T. cruzi* along the cell cycle (Fig. 2, panel B), and given the relatively mild effects of RNAi in procyclic cells, a direct role in the cell cycle control cannot be ascertained. Given the strength of the phenotype in the procyclic form, future work will involve the generation of a procyclic conditional knockout cell line. In addition, it is worth pointing out that RNAi-mediated downregulation of *Tb*Pin1 and *Tb*Par14 did not abolish cell proliferation (data not shown).

One of the most intriguing questions is what the exact physiological role of Par45 is, since this multi-domain parvulin has been described in a small number of organisms. Interestingly, from the studies on these multi-domain proteins, it can be argued that the involvement of the PPIase domain in a given process is possibly related to the functional properties of the accompanying FHA domain. In *h*Pin1, a common WW protein–protein interaction module is linked to a C-terminal PPIase domain [4]. Early structure-to-function analyses have revealed that the unique substrate specificity of Pin1 towards specific pSer/Thr-Pro motifs results from interactions provided by both of these domains, which form a 'double-check' mechanism ([4] and references therein). In Par45, both domains seem to function independently. Taking into account that in Par45 the protein–protein interaction FHA domain is coupled to a PPIase domain, it seems plausible that the two domains could act on different motifs on the same target protein. Intriguingly, whereas FHA is a pThr-binding module, the catalytic PPIase domain of Par45 displayed substrate specificity towards Arg-Pro motifs to regulate protein function by controlling their conformations. Recent works have shown that the FHA domains of NIPP1 and other FHA-containing proteins preferentially bind pThr-Pro-containing peptide stretches [47–49]. This striking characteristic places the FHA domain in a

growing class of domains that recognize pThr-Pro motifs that include the WW domain found in Pin1-type PPIases. It would be interesting to determine whether the FHA domain of Par45 uses a common mechanism of Pro recognition at this position.

In conclusion, we identified and biochemically characterized a novel parvulin-type PPIase from the evolutionary divergent *T. cruzi*. Our results reveal an unexpected substrate specificity of the Par45 enzyme. The presence of PPIases in trypanosomes, together with the presence of the atypical *Tc*Par45, underscores the importance of prolyl *cis*/*trans* isomerization in various biological processes during the life of trypanosomes. Furthermore, given that there are orthologs in *L. major* and *T. brucei*, the role of Par45 requires further investigation.

Acknowledgments

We thank Prof. Dr. Gunter Fischer and Dr. Cordelia Schiene-Fischer for their assistance, G. Prat Gay and A. Heer for the Maldi analysis. E. E. thanks the DAAD for a fellowship with the student exchange program. The work was supported by Consejo Nacional de Investigaciones Científicas y Técnicas (CONICET, Argentina) and Agencia Nacional de Promoción Científica y Tecnológica (ANPCyT, Argentina). Part of this work was supported by grants from Prosul-CNPq and FAPESP (Brazil).

Appendix A. Supplementary data

Supplementary data associated with this article can be found, in the online version, at doi:10.1016/j.bbamcr.2010.05.006.

References

[1] C. Schiene, G. Fischer, Enzymes that catalyse the restructuring of proteins, Curr. Opin. Struct. Biol. 10 (2000) 40–45.
[2] K.P. Lu, G. Finn, T.H. Lee, L.K. Nicholson, Prolyl *cis-trans* isomerization as a molecular timer, Nat. Chem. Biol. 3 (2007) 619–629.
[3] G. Fischer, T. Aumuller, Regulation of peptide bond *cis*/*trans* isomerization by enzyme catalysis and its implication in physiological processes, Rev. Physiol. Biochem. Pharmacol. 148 (2003) 105–150.
[4] K.P. Lu, S.D. Hanes, T. Hunter, A human peptidyl-prolyl isomerase essential for regulation of mitosis, Nature 380 (1996) 544–547.
[5] R. Ranganathan, K.P. Lu, T. Hunter, J.P. Noel, Structural and functional analysis of the mitotic rotamase Pin1 suggests substrate recognition is phosphorylation dependent, Cell 89 (1997) 875–886.
[6] M.B. Yaffe, M. Schutkowski, M. Shen, X.Z. Zhou, P.T. Stukenberg, J.U. Rahfeld, J. Xu, J. Kuang, M.W. Kirschner, G. Fischer, L.C. Cantley, K.P. Lu, Sequence-specific and phosphorylation-dependent proline isomerization: a potential mitotic regulatory mechanism, Science 278 (1997) 1957–1960.
[7] M. Shen, P.T. Stukenberg, M.W. Kirschner, K.P. Lu, The essential mitotic peptidyl-prolyl isomerase Pin1 binds and regulates mitosis-specific phosphoproteins, Genes Dev. 12 (1998) 706–720.
[8] X. Zhou, O. Kops, A. Werner, P. Lu, M. Shen, G. Stoller, G. Kullertz, M. Stark, G. Fischer, K. Lu, Pin1-dependent prolyl isomerization regulates dephosphorylation of Cdc25C and tau proteins, Mol. Cell 6 (2000) 873–883.
[9] J. Hani, B. Schelbert, A. Bernhardt, H. Domdey, G. Fischer, K. Wiebauer, J. Rahfeld, Mutations in a peptidyl prolyl-*cis*/*trans*-isomerase gene lead to a defect in 3′-end formation of a pre-mRNA in *Saccharomyces cerevisiae*, J. Biol. Chem. 274 (1999) 108–116.
[10] I. Landrieu, L. De Veylder, J.S. Fruchart, B. Odaert, P. Casteels, D. Portetelle, M. Van Montagu, D. Inze, G. Lippens, The *Arabidopsis thaliana* PIN1At gene encodes a single-domain phosphorylation-dependent peptidyl prolyl cis/trans isomerase, J. Biol. Chem. 275 (2000) 10577–10581.
[11] M. Metzner, G. Stoller, K.P. Rucknagel, K.P. Lu, G. Fischer, M. Luckner, G. Kullertz, Functional replacement of the essential ESS1 in yeast by the plant parvulin DlPar13, J. Biol. Chem. 276 (2001) 13524–13529.
[12] J.L. Yao, O. Kops, P.J. Lu, K.P. Lu, Functional conservation of phosphorylation-specific prolyl isomerases in plants, J. Biol. Chem. 276 (2001) 13517–13523.
[13] T. Uchida, F. Fujimori, T. Tradler, G. Fischer, J.U. Rahfeld, Identification and characterization of a 14 kDa human protein as a novel parvulin-like peptidyl prolyl cis/trans isomerase, FEBS Lett. 446 (1999) 278–282.
[14] M. Sudol, Structure and function of the WW domain, Prog. Biophys. Mol. Biol. 65 (1996) 113–132.
[15] J.F. Rippmann, S. Hobbie, C. Daiber, B. Guilliard, M. Bauer, J. Birk, H. Nar, P. Garin-Chesa, W.J. Rettig, A. Schnapp, Phosphorylation-dependent proline isomerization catalyzed by Pin1 is essential for tumor cell survival and entry into mitosis, Cell Growth Differ. 11 (2000) 409–416.
[16] Y.X. Xu, Y. Hirose, X.Z. Zhou, K.P. Lu, J.L. Manley, Pin1 modulates the structure and function of human RNA polymerase II, Genes Dev. 17 (2003) 2765–2776.
[17] Y.X. Xu, J.L. Manley, Pin1 modulates RNA polymerase II activity during the transcription cycle, Genes Dev. 21 (2007) 2950–2962.
[18] C.B. Wilcox, A. Rossettini, S.D. Hanes, Genetic interactions with C-terminal domain (CTD) kinases and the CTD of RNA Pol II suggest a role for ESS1 in transcription initiation and elongation in *Saccharomyces cerevisiae*, Genetics 167 (2004) 93–105.
[19] X. Wu, A. Rossettini, S.D. Hanes, The ESS1 prolyl isomerase and its suppressor BYE1 interact with RNA Pol II to inhibit transcription elongation in *Saccharomyces cerevisiae*, Genetics 165 (2003) 1687–1702.
[20] T.A. Surmacz, E. Bayer, J.U. Rahfeld, G. Fischer, P. Bayer, The N-terminal basic domain of human parvulin hPar14 is responsible for the entry to the nucleus and high-affinity DNA-binding, J. Mol. Biol. 321 (2002) 235–247.
[21] T. Reimer, M. Weiwad, A. Schierhorn, P.K. Ruecknagel, J.U. Rahfeld, P. Bayer, G. Fischer, Phosphorylation of the N-terminal domain regulates subcellular localization and DNA binding properties of the peptidyl-prolyl cis/trans isomerase hPar14, J. Mol. Biol. 330 (2003) 955–966.
[22] T. Uchida, M. Takamiya, M. Takahashi, H. Miyashita, H. Ikeda, T. Terada, Y. Matsuo, M. Shirouzu, S. Yokoyama, F. Fujimori, T. Hunter, Pin1 and Par14 peptidyl prolyl isomerase inhibitors block cell proliferation, Chem. Biol. 10 (2003) 15–24.
[23] S. Fujiyama-Nakamura, H. Yoshikawa, K. Homma, T. Hayano, T. Tsujimura-Takahashi, K. Izumikawa, H. Ishikawa, N. Miyazawa, M. Yanagida, Y. Miura, T. Shinkawa, Y. Yamauchi, T. Isobe, N. Takahashi, Parvulin (Par14), a peptidyl-prolyl cis-trans isomerase, is a novel rRNA processing factor that evolved in the metazoan lineage, Mol. Cell Proteomics 8 (2009) 1552–1565.
[24] E.D. Erben, S. Daum, M.T. Tellez-Inon, The *Trypanosoma cruzi* PIN1 gene encodes a parvulin peptidyl-prolyl cis/trans isomerase able to replace the essential ESS1 in *Saccharomyces cerevisiae*, Mol. Biochem. Parasitol. 153 (2007) 186–193.
[25] A. Dereeper, V. Guignon, G. Blanc, S. Audic, S. Buffet, F. Chevenet, J.F. Dufayard, S. Guindon, V. Lefort, M. Lescot, J.M. Claverie, O. Gascuel, Phylogeny.fr: robust phylogenetic analysis for the non-specialist, Nucleic Acids Res. 36 (2008) W465–469.
[26] N. Saitou, M. Nei, The neighbor-joining method: a new method for reconstructing phylogenetic trees, Mol. Biol. Evol. 4 (1987) 406–425.
[27] B. Janowski, S. Wollner, M. Schutkowski, G. Fischer, A protease-free assay for peptidyl prolyl *cis*/*trans* isomerases using standard peptide substrates, Anal. Biochem. 252 (1997) 299–307.
[28] X. Wu, C.B. Wilcox, G. Devasahayam, R.L. Hackett, M. Arevalo-Rodriguez, M.E. Cardenas, J. Heitman, S.D. Hanes, The Ess1 prolyl isomerase is linked to chromatin remodeling complexes and the general transcription machinery, EMBO J. 19 (2000) 3727–3738.
[29] M.J.B. van den Hoff, A.F.M. Moorman, W.H. Lamers, Electroporation in 'intracellular' buffer increases cell survival, Nucl. Acids Res. 20 (1992) 2902.
[30] Z. Wang, J.C. Morris, M.E. Drew, P.T. Englund, Inhibition of *Trypanosoma brucei* gene expression by RNA interference using an integratable vector with opposing T7 promoters, J. Biol. Chem. 275 (2000) 40174–40179.
[31] E. Wirtz, S. Leal, C. Ochatt, G.A. Cross, A tightly regulated inducible expression system for conditional gene knock-outs and dominant-negative genetics in *Trypanosoma brucei*, Mol. Biochem. Parasitol. 99 (1999) 89–101.
[32] S. Shen, G.K. Arhin, E. Ullu, C. Tschudi, *In vivo* epitope tagging of *Trypanosoma brucei* genes using a one step PCR-based strategy, Mol. Biochem. Parasitol. 113 (2001) 171–173.
[33] N. Galanti, J.A. Dvorak, J. Grenet, J.P. McDaniel, Hydroxyurea-induced synchrony of DNA replication in the Kinetoplastida, Exp. Cell Res. 214 (1994) 225–230.
[34] G. Fischer, Peptidyl-prolyl *cis*/*trans* isomerases and their effectors, Angewandte Chemie International Edition, 33, 1994, pp. 1415–1436.
[35] K. Hofmann, P. Bucher, The FHA domain: a putative nuclear signalling domain found in protein kinases and transcription factors, Trends Biochem. Sci. 20 (1995) 347–349.
[36] C.D. Behrsin, M.L. Bailey, K.S. Bateman, K.S. Hamilton, L.M. Wahl, C.J. Brandl, B.H. Shilton, D.W. Litchfield, Functionally important residues in the peptidyl-prolyl isomerase Pin1 revealed by unigenic evolution, J. Mol. Biol. 365 (2007) 1143–1162.
[37] L. Hennig, C. Christner, M. Kipping, B. Schelbert, K. Rucknagel, S. Grabley, G. Kullertz, G. Fischer, Selective inactivation of parvulin-like peptidyl-prolyl *cis*/*trans* isomerases by juglone, Biochemistry 37 (1998) 5953–5960.
[38] E. Sekerina, J.U. Rahfeld, J. Muller, J. Fanghanel, C. Rascher, G. Fischer, P. Bayer, NMR solution structure of hPar14 reveals similarity to the peptidyl prolyl *cis*/*trans* isomerase domain of the mitotic regulator hPin1 but indicates a different functionality of the protein, J. Mol. Biol. 301 (2000) 1003–1017.
[39] T. Terada, M. Shirouzu, Y. Fukumori, F. Fujimori, Y. Ito, T. Kigawa, S. Yokoyama, T. Uchida, Solution structure of the human parvulin-like peptidyl prolyl *cis*/*trans* isomerase, hPar14, J. Mol. Biol. 305 (2001) 917–926.
[40] V. Bellofatto, J.B. Palenchar, RNA interference as a genetic tool in trypanosomes, Methods Mol. Biol. 442 (2008) 83–94.
[41] W.D. DaRocha, K. Otsu, S.M. Teixeira, J.E. Donelson, Tests of cytoplasmic RNA interference (RNAi) and construction of a tetracycline-inducible T7 promoter system in *Trypanosoma cruzi*, Mol. Biochem. Parasitol. 133 (2004) 175–186.
[42] P. Lu, X. Zhou, M. Shen, K. Lu, Function of WW domains as phosphoserine- or phosphothreonine-binding modules, Science 283 (1999) 1325–1328.
[43] P.J. Lu, X.Z. Zhou, Y.C. Liou, J.P. Noel, K.P. Lu, Critical role of WW domain phosphorylation in regulating phosphoserine binding activity and Pin1 function, J. Biol. Chem. 277 (2002) 2381–2384.
[44] J.U. Rahfeld, K.P. Rucknagel, B. Schelbert, B. Ludwig, J. Hacker, K. Mann, G. Fischer, Confirmation of the existence of a third family among peptidyl-prolyl *cis*/*trans*

isomerases. Amino acid sequence and recombinant production of parvulin, FEBS Lett. 352 (1994) 180–184.
[45] M.P. Vazquez, M.J. Levin, Functional analysis of the intergenic regions of TcP2beta gene loci allowed the construction of an improved *Trypanosoma cruzi* expression vector, Gene 239 (1999) 217–225.
[46] T.R. Gemmill, X. Wu, S.D. Hanes, Vanishingly low levels of Ess1 prolyl-isomerase activity are sufficient for growth in *Saccharomyces cerevisiae*, J. Biol. Chem. 280 (2005) 15510–15517.
[47] H. Li, I.J. Byeon, Y. Ju, M.D. Tsai, Structure of human Ki67 FHA domain and its binding to a phosphoprotein fragment from hNIFK reveal unique recognition sites and new views to the structural basis of FHA domain functions, J. Mol. Biol. 335 (2004) 371–381.
[48] A. Boudrez, M. Beullens, E. Waelkens, W. Stalmans, M. Bollen, Phosphorylation-dependent interaction between the splicing factors SAP155 and NIPP1, J. Biol. Chem. 277 (2002) 31834–31841.
[49] D. Reynolds, B.J. Shi, C. McLean, F. Katsis, B. Kemp, S. Dalton, Recruitment of Thr 319-phosphorylated Ndd1p to the FHA domain of Fkh2p requires Clb kinase activity: a mechanism for CLB cluster gene activation, Genes Dev. 17 (2003) 1789–1802.
[50] S.D. Hanes, P.R. Shank, K.A. Bostian, Sequence and mutational analysis of ESS1, a gene essential for growth in *Saccharomyces cerevisiae*, Yeast 5 (1989) 55–72.
[51] K. Lu, S. Hanes, T. Hunter, A human peptidyl-prolyl isomerase essential for regulation of mitosis, Nature 380 (1996) 544–547.
[52] J.U. Rahfeld, A. Schierhorn, K. Mann, G. Fischer, A novel peptidyl-prolyl *cis*/*trans* isomerase from *Escherichia coli*, FEBS Lett. 343 (1994) 65–69.